⌘ Author's Choice

© 2011 by The American Society for Biochemistry and Molecular Biology, Inc.
This paper is available on line at http://www.mcponline.org

High Throughput Isolation and Glycosylation Analysis of IgG–Variability and Heritability of the IgG Glycome in Three Isolated Human Populations*[S]

Maja Pučić‡, Ana Knežević‡, Jana Vidič§, Barbara Adamczyk¶, Mislav Novokmet‡, Ozren Polašek‖, Olga Gornik, Sandra Šupraha-Goreta**, Mark R. Wormald‡‡, Irma Redžić**, Harry Campbell§§, Alan Wright¶¶, Nicholas D. Hastie¶¶, James F. Wilson§§, Igor Rudan‖§§, Manfred Wuhrer‖‖, Pauline M. Rudd¶, Djuro Josić[ab], and Gordan Lauc‡**[c]**

All immunoglobulin G molecules carry *N*-glycans, which modulate their biological activity. Changes in *N*-glycosylation of IgG associate with various diseases and affect the activity of therapeutic antibodies and intravenous immunoglobulins. We have developed a novel 96-well protein G monolithic plate and used it to rapidly isolate IgG from plasma of 2298 individuals from three isolated human populations. *N*-glycans were released by PNGase F, labeled with 2-aminobenzamide and analyzed by hydrophilic interaction chromatography with fluorescence detection. The majority of the structural features of the IgG glycome were consistent with previous studies, but sialylation was somewhat higher than reported previously. Sialylation was particularly prominent in core fucosylated glycans containing two galactose residues and bisecting GlcNAc where median sialylation level was nearly 80%. Very high variability between individuals was observed, approximately three times higher than in the total plasma glycome. For example, neutral IgG glycans without core fucose varied between 1.3 and 19%, a difference that significantly affects the effector functions of natural antibodies, predisposing or protecting individuals from particular diseases. Heritability of IgG glycans was generally between 30 and 50%. The individual's age was associated with a significant decrease in galactose and increase of bisecting GlcNAc, whereas other functional elements of IgG glycosylation did not change much with age. Gender was not an important predictor for any IgG glycan. An important observation is that competition between glycosyltransferases, which occurs *in vitro*, did not appear to be relevant *in vivo*, indicating that the final glycan structures are not a simple result of competing enzymatic activities, but a carefully regulated outcome designed to meet the prevailing physiological needs. ***Molecular & Cellular Proteomics 10: 10.1074/mcp.M111.010090, 1–15, 2011.***

From the ‡Genos Ltd., Glycobiology Division, Planinska 1, 10000 Zagreb, Croatia; §BIA Separations Ltd., Teslova 30, 1000 Ljubljana, Slovenia; ¶National Institute for Bioprocessing Research and Training, Dublin-Oxford Glycobiology Laboratory, Conway Institute, University College Dublin, Belfield, Dublin 4, Ireland; ‖University of Split School of Medicine, Šoltanska 2, Split, Croatia; **University of Zagreb, Faculty of Pharmacy and Biochemistry, Ante Kovačića 1, 10000 Zagreb, Croatia; ‡‡Oxford Glycobiology Institute, Department of Biochemistry, University of Oxford, Oxford, UK; §§Centre for Population Health Sciences, The University of Edinburgh Medical School, Edinburgh, UK; ¶¶MRC Human Genetics Unit; Institute of Genetics and Molecular Medicine, Western General Hospital, Edinburgh, UK; ‖‖Biomolecular Mass Spectrometry Unit, Department of Parasitology, Leiden University Medical Center, Leiden, The Netherlands; [a]COBRE Center for Cancer Research Development, Rhode Island Hospital and Brown University, Providence, RI 02903; [b]Department of Biotechnology, University of Rijeka, Trg Braće Mažuranića 10, 51 000 Rijeka, Croatia

[S] This article contains supplemental Tables S1 and S2.

Received April 6, 2011, and in revised form, June 6, 2011

⌘ *Author's Choice*—Final version full access.

Published, MCP Papers in Press, June 8, 2011, DOI 10.1074/mcp.M111.010090

Glycosylation is a widespread post-translational modification capable of producing significant structural changes to proteins. Contrary to the core *N*-glycan structure, which is essential for multicellular life (1), mutations in genes involved in modifications of glycan antennae are common and cause a large part of individual phenotypic variations that exist in humans and other higher organisms. Glycosylation of membrane receptors modulates adaptive properties of the cell membrane and affects communication between the cell and its environment (2). Deregulation of glycosylation is associated with a wide range of diseases, including cancer, diabetes, cardiovascular, congenital, immunological and infectious disorders (3–5). Variations in glycosylation are of great physiological significance because it has been demonstrated that changes in glycans significantly modulate the structure and function of polypeptide parts of glycoproteins (6), and a prom-

inent example for this type of regulation is the immunoglobulin G (IgG).

Each heavy chain of IgG carries a single covalently attached bi-antennary *N*-glycan at the highly conserved asparagine 297 residue in each of the C_H2 domains of the Fc region of the molecule. The attached oligosaccharides are structurally important for the stability of the antibody and its effector functions (7). In addition, 15–20% of normal IgG molecules also bear complex bi-antennary oligosaccharides attached to the variable regions of the light chain, heavy chain or both (8, 9). Decreased galactosylation of IgG glycans in rheumatoid arthritis was reported over 25 years ago (10) and numerous subsequent studies of IgG glycosylation revealed a number of important functional consequences of structural alterations in IgG glycans. For example, the addition of sialic acids dramatically changes the physiological role of IgGs by converting them from pro-inflammatory into anti-inflammatory agents (11, 12). Another structural change to IgG glycans, the addition of fucose to the glycan core, interferes with binding of IgG to FcγRIIIa and dampens its ability to destroy target cells through antibody dependent cell-mediated cytotoxicity (ADCC) (13, 14). Lack of core fucose enhances the clinical efficacy of monoclonal antibodies, which exert their therapeutic effect by ADCC mediated killing (15–17). However, despite the undisputed importance of glycosylation for the function of IgGs, a large scale study that identifies the variability and heritability of IgG glycosylation in human populations has not been attempted.

One of the major bottlenecks in large scale proteomics and glycomics studies is protein purification from a large number of samples. Affinity chromatography and liquid chromatography have been widely used, as they are versatile techniques for this purpose. A combination of affinity chromatography and monolithic supports exhibits many advantageous properties when compared with conventional particulate supports (18–22). Monoliths are continuous stationary phases cast in a single piece with very large and highly interconnected pores (23). In comparison to particulate supports where molecules are transferred by diffusion, the high porosity of monoliths allows convective mass transport. This makes resolution and dynamic binding capacity practically independent of the flow rate (24–27). High dynamic binding capacity for large molecules and high flow rates at a very low pressure drop enable rapid processing of large volumes of complex biological mixtures (28). Polymethacrylate monoliths, specifically poly(glycidyl methacrylate-*co*-ethylene dimethacrylate), possess all of the above mentioned characteristics of monolithic supports. In addition, they are also known for their good mechanical strength, pH resistance, high surface area, high porosity, and simple attachment of ligands to the epoxy groups (29). One of the most commonly used bioaffinity ligands for the isolation of IgG is protein G (30–32). All four subclasses of human IgG strongly bind to protein G through their Fc fragments. Here we present the development and application of a 96-well Protein G monolithic plate for high throughput isolation of IgG and its application for the first large scale population study of the IgG glycome.

EXPERIMENTAL PROCEDURES

Chemicals—Glycidyl methacrylate, ethylene dimethacrylate, cyclohexanol, and 1-dodecanol were purchased from Sigma-Aldrich (St. Louis, MO). Photoinitiator was purchased from CIBA (Basel, Switzerland) and Protein G from GE Healthcare (Uppsala, Sweden). Sodium acetate, sulfuric acid, and hydrochloric acid (37%) were obtained from Merck (Darmstadt, Germany). All the buffers were filtered through a 0.45 μm pore size filter composed of Sartolon polyamide (Sartorius, Goettingen, Germany). The 96-well plates with frits, mean pore size 36 microns, were purchased from Chromacol (Welwyn Garden City, United Kingdom).

Chemicals for buffer preparations (phosphate buffered saline (PBS), Tris, HCl, NaOH, formic acid, ammonium bicarbonate, propan-2-ol) were purchased from Fisher Scientific (Pittsburgh, PA) and Sigma-Aldrich. Chemicals for running the SDS-PAGE were purchased from Invitrogen (Carlsbad, CA). Sodium bicarbonate, DL-dithiothreitol, iodoacetamide, ammonium persulfate, 2-aminobenzamide, sodium cyanoborohydride, acetic acid, and dimethyl sulfoxide were from Sigma-Aldrich and ultra pure water (Purite Fusion 40 water purification system, Purite Ltd., Thame, UK) were used throughout.

Human Samples—This study was based on samples from respondents who were residents of the Croatian Adriatic islands Vis and Korčula or the Northern Scottish Orkney Islands and who were recruited within a larger genetic epidemiology program that sought to investigate genetic variability and map genes influencing common complex diseases and disease traits in genetically isolated populations (33, 34). The genetic-epidemiology program on the islands began in 2002, and continues today. The sampling framework was based on the voting register in Croatia, which was used to send postal invitations to all adult inhabitants (over 18 years of age); in Orkney subjects were volunteers from the Orkney Complex Disease Study, again aged over 18 years.

The sample for this study consisted of 906 subjects from the Vis island (39.4%), 915 (39.8%) from Korčula island and 477 from the Orkney islands (20.8%) totaling to 2298 individuals. The age range for the entire sample was 18–100 years (median age 56, interquartile range 22 years). There were 894 men (39.2%) and 1384 women in the sample (60.8%), for 20 people gender data were missing. Heritability analysis was performed for the Vis Island sample only, because of a more extensive number of familial links. The genealogical information was reconstructed based on the Church Parish records and information provided by the subjects, and then checked against genetic data on allele sharing between relatives as a quality control measure to exclude data errors. The sample contained a total of 809 genealogical relationships (including 205 parent-child, 123 sibling, and 481 other relationships). The Korčula sample contained a much lower number of familial links and because of large standard errors arising from rather shallow genealogical records, we did not calculate heritability estimates for the Korčula island sample.

All of the members of the three sample groups were interviewed by one of the trained surveyors, based on an extensive questionnaire (35). The questionnaire collected data on personal characteristics (name, date, and place of birth, gender, marital status, education level and occupation), selected health-related lifestyle variables (such as diet and smoking status), health complaints, drug intake and hospitalization records. Blood was taken in epruvetes containing anticoagulant and immediately processed; plasma was separated by centrifugation and stored at −70 °C. This study conformed to the ethical guidelines of the 1975 Declaration of Helsinki. All respondents signed

an informed consent form before participating in the study and the study was approved by the appropriate Ethics Board of the University of Zagreb Medical School and by Research Ethics Committees in Orkney and Aberdeen.

Preparation of Protein G Monolithic Plates—The 96-well plates consisting of a polymethacrylate (poly(glycidyl methacrylate-*co*-ethylene dimethacrylate)) monolithic stationary phase with protein G coupled to the epoxy groups and casted inside each well was custom designed and prepared by BIA Separations (Ljubljana, Slovenia). The basic monolith was synthesized by a free-radical polymerization of GMA and a cross-linking agent, EDMA, in the presence of porogenic solvents, cyclohexanol and dodecanol (60 vol.% of the reaction mixture) as described by Tennikova *et al.* (36), but instead of thermally initiated polymerization, UV polymerization was used. The preparation of the monolithic stationary phase is a simple process and the polymerization mixture, which consists of monomers and porogens, is polymerized by applying heat and UV light. In both types of polymerization, an important property of a monolithic macroporous material is the pore size distribution. The photoinduced copolymerization of 150 μl of the mixtures of monomers, cross-linking agent, photoinitiator, and porogenic solvents was performed at room temperature directly in each well of 96 plates. The mixture was irradiated with a constant intensity from a 5 $\times$ 8 W mercury lamp using a wavelength of 312 nm (UVItec Ltd, Cambridge, UK) with an exposure time of up to 180 min. Although the instrument does not enable active cooling, the temperature did not exceed 30 °C thus effectively excluding thermal initiation. After the polymerization was completed, each well of the 96-well plate was extensively washed with ethanol to wash out the porogenic solvents and other soluble compounds. The average pore size was determined by intrusive mercury porosimetry (PASCAL 440 porosimeter, Thermoquest Italia, Rodano, Italy). The pore size distribution of the monoliths were around 700 nm, which is comparable to thermally polymerized monoliths (37). The immobilization of protein G on the monoliths in the 96-well plate was performed by flushing the monoliths with protein G solution prepared in a buffer solution of sodium acetate. Afterward the monoliths were flushed with deionized water and the deactivation of the remaining epoxy groups was performed with 0.5 M solution of sulfuric acid.

Isolation of IgG—Before use, the monolithic plate was washed with 10 column volumes (CV) of ultra pure water and then equilibrated with 10 CV of binding buffer (1X PBS, pH 7.4). Plasma samples (50 μl) were diluted 10 $\times$ with the binding buffer and applied to the Protein G plate. The filtration of the samples was completed in ~5 min. The plate was then washed five times with 5 CV of binding buffer to remove unbound proteins. IgG was released from the protein G monoliths using 5 CV of elution solvent (0.1 M formic acid, pH 2.5). Eluates were collected in a 96-deep-well plate and immediately neutralized to pH 7.0 with neutralization buffer (1 M ammonium bicarbonate) to maintain the IgG stability. After each sample application, the monoliths were regenerated with the following buffers: 10 CV of 10 $\times$ PBS, followed by 10 CV of 0.1 M formic acid and afterward 10 CV of 1 $\times$ PBS to re-equilibrate the monoliths. Each step of the chromatographic procedure was done under vacuum (cca. 60 mmHg pressure reduction while applying the samples, 500 mmHg during elution and washing steps) using a manual set-up consisting of a multichannel pipet, a vacuum manifold (Beckman Coulter, Brea, CA) and a vacuum pump (Pall Life Sciences, Ann Arbor, MI). If the plate was not used for a short period, it was stored in 20% ethanol (v/v) at 4 °C.

After repeated use of the plate contaminants present in the sample sometimes did not completely elute from the monolithic stationary phase. A specific cleaning protocol was developed that included washing with 0.1 M NaOH to remove precipitated proteins and with 30% propan-2-ol to remove strongly bound hydrophobic proteins or lipids. This procedure effectively removed all precipitates and did not significantly diminish IgG binding capacity of the immobilized protein G.

The purity of the isolated IgG was verified by SDS-PAGE with NuPAGE Novex 4–12% Bis-Tris gels in an Xcell SureLock Mini-Cell (Invitrogen) according to the manufacturer. Precision Plus Protein All Blue Standards (BioRad, Hercules, CA) was used as the molecular weight marker. The gels were run at 180 V for 45 min, stained with GelCode Blue (Pierce) and visualized by a VersaDoc Imaging System (BioRad).

Glycan Release and Labeling—Glycan release and labeling was performed as reported previously (38). Plasma proteins were immobilized in a block of SDS-polyacrylamide gel and *N*-glycans were released by digestion with recombinant N-glycosidase F (ProZyme, CA). This was done in a 96-well microtiter plate to achieve the best throughput of sample preparation. After extraction, glycans were fluorescently labeled with 2-aminobenzamide.

Exoglycosidase Digestions of 2-AB Labeled IgG N-Glycans—The following enzymes, all purchased from ProZyme (San Leandro, CA), were used for digestions: Sialidase A™/NANase III (recombinant gene from *Arthrobacter ureafaciens*, expressed in *Escherichia coli*), 5 mU; α(1–2,3,4,6)fucosidase (bovine kidney), 1.25 mU; α(1–3,4)-fucosidase (almond meal), 1.6 mU; β(1–3,4)-galactosidase (bovine testis), 5 mU; β(1–4)-galactosidase (*Streptococcus pneumoniae*), 2 mU; β-N-acetylhexosaminidase/HEXase I (recombinant gene from *Streptococcus pneumoniae*, expressed in *E. coli*), 40 mU; α(1–2,3,6)-mannosidase (jack bean), 150 mU. Aliquots of the 2-AB labeled glycan pool were dried down and digested in a mixture of enzymes, corresponding 1X concentrated manufacturers buffer and water in total volume of 5 μl. After overnight incubation at 37 °C, enzymes were removed by filtration through the AcroPrep 96 Filter Plates, 10K (Pall Corporation, MI, USA). Digested glycans were then separated by HILIC-UPLC for comparison against an undigested equivalent.

Hydrophilic Interaction Chromatography—Fluorescently labeled *N*-glycans were separated by ultra performance liquid chromatography on a Waters Acquity UPLC instrument consisting of a quaternary solvent manager, sample manager and a FLR fluorescence detector set with excitation and emission wavelengths of 330 and 420 nm, respectively. The instrument was under the control of Empower 2 software, build 2145 (Waters, Milford, MA). Labeled *N*-glycans were separated on a Waters BEH Glycan chromatography column, 100 $\times$ 2.1 mm i.d., 1.7 μm BEH particles, with 100 mM ammonium formate, pH 4.4, as solvent A and acetonitrile as solvent B. Recently reported methods for UPLC profiling of glycans (39, 40) were used as a starting point for the development of the separation method that used linear gradient of 75–62% acetonitrile at flow rate of 0.4 ml/min in a 20 min analytical run. Samples were maintained at 5 °C before injection, and the separation temperature was 60 °C. The system was calibrated using an external standard of hydrolyzed and 2-AB labeled glucose oligomers from which the retention times for the individual glycans were converted to glucose units. Data processing was performed using an automatic processing method with a traditional integration algorithm after which each chromatogram was manually corrected to maintain the same intervals of integration for all the samples. The chromatograms obtained were all separated in the same manner into 24 peaks and the amount of glycans in each peak was expressed as % of total integrated area.

MS Analysis of Glycans—Before MS analysis of each glycan peak, the 2-AB labeled IgG *N*-glycan pool was fractionated by hydrophilic interaction high performance liquid chromatography (HILIC) on a 100 $\times$ 2.1 mm i.d., 1.7 μm BEH particles column using a linear gradient of 75–62% acetonitrile with 100 mM ammonium formate, pH 4.4, as solvent A and acetonitrile as solvent B. UltiMate Dual Gradient LC system (Dionex, Sunnyvale, CA) controlled by Chromeleon soft-

ware and connected to *FP-2020* Plus fluorescence detector (Jasco, Easton, MD) was used. To obtain the same separation as with UPLC system, flow was adjusted to 0.3 ml/min and analytical run time was prolonged to 60 min. Collected fractions were dried by vacuum centrifugation and resuspended in water.

Nano-LC-ESI-MS/MS. MS analysis of the collected glycan fractions was performed using an Ultimate 3000 nano-LC system (Dionex/LC Packings, Amsterdam, The Netherlands) equipped with a reverse phase trap column (C_{18} PepMap 100Å, 5 μm, 300 μm $\times$ 5 mm; Dionex/LC Packings) and a nano column (C_{18} PepMap 100Å, 3 μm, 75 μm $\times$ 150 mm; Dionex/LC Packings).

The column was equilibrated at room temperature with eluent A (0.1% formic acid in water) at a flow rate of 300 nL/min. For fractions with disialylated glycans, extra 0.04% of trifluoroacetic acid was added to the eluent A. After injection of the samples, a gradient was applied to 25% eluent B (95% acetonitrile) in 15 min and to 70% eluent B at 25 min followed by an isocratic elution with 70% eluent B for 5 min. The eluate was monitored by UV absorption at 214 nm. The LC system was coupled *via* an online nanospray source to an Esquire HCTultra ESI-IT-MS (Bruker Daltonics, Bremen, Germany) operated in the positive ion mode. For electrospray (1100–1250 V), stainless steel capillaries with an inner diameter of 30 μm (Proxeon, Odense, Denmark) were used. The solvent was evaporated at 170 °C employing a nitrogen stream of 7 L/min. Ions from *m/z* 500 to 1800 were registered. Automatic fragment ion analysis was enabled, resulting in MS/MS spectra of the most abundant ions in the MS spectra. Glycan structures were assigned using GlycoWorkbench (41).

MALDI-TOF-MS. 2-AB labeled glycan fractions were spotted onto an AnchorChip target plate (Bruker Daltonics, Bremen, Germany). Subsequently 1 μl of 5 mg/ml 2,5-dihydroxybenzoic acid in 50% acetonitrile was applied on top of each sample and allowed to dry at room temperature. MALDI-TOF-MS was performed on an UltrafleX II mass spectrometer (Bruker Daltonics). Calibration was performed on a peptide calibration standard. Spectra were acquired in reflector positive mode over the *m/z* range from 700 to 3500 Da for a total of 2000 shots. Glycan structures were assigned using GlycoWorkbench (41).

Calculation of Derived Glycosylation Traits—Derived glycosylation traits were approximated from the ratios of glycan peaks (GP1-GP24) each of which combined the glycans with the same structural characteristics (see Table I). The minor glycan peak GP3 was excluded from all the calculations because in some samples it co-eluted with a contaminant that significantly affected its value. Derived traits were defined as: the percentage of sialylation of fucosylated galactosylated structures without bisecting GlcNAc in total IgG glycans-FGS/(FG + FGS) = SUM(GP16 + GP18 + GP23)/SUM(GP16 + GP18 + GP23 + GP8 + GP9 + GP14)* 100; the percentage of sialylation of fucosylated galactosylated structures with bisecting GlcNAc in total IgG glycans-FBGS/(FBG + FBGS) = SUM(GP19 + GP24)/SUM(GP19 + GP24 + GP10 + GP11 + GP15)* 100; the percentage of sialylation of all fucosylated structures without bisecting GlcNAc in total IgG glycans-FGS/(F + FG + FGS) = SUM(GP16 + GP18 + GP23)/SUM(GP16 + GP18 + GP23 + GP4 + GP8 + GP9 + GP14)* 100; the percentage of sialylation of all fucosylated structures with bisecting GlcNAc in total IgG glycans-FBGS/(FB + FBG + FBGS) = SUM(GP19 + GP24)/SUM(GP19 + GP24 + GP6 + GP10 + GP11 + GP15)* 100; the percentage of monosialylation of fucosylated monogalactosylated structures in total IgG glycans-FG1S1/(FG1 + FG1S1) = GP16/SUM(GP16 + GP8 + GP9)* 100; the percentage of monosialylation of fucosylated digalactosylated structures in total IgG glycans-FG2S1/(FG2+FG2S1+FG2S2) = GP18/SUM(GP18 + GP14 + GP23)* 100; the percentage of disialylation of fucosylated digalactosylated structures in total IgG glycans-FG2S2/(FG2 + FG2S1 + FG2S2) = GP23/SUM(GP23 + GP14 + GP18)* 100; the percentage of monosialylation of fucosylated digalactosylated structures with bisecting GlcNAc in total IgG glycans-FBG2S1/(FBG2 + FBG2S1 + FBG2S2) = GP19/SUM(GP19 + GP15 + GP24)* 100; the percentage of disialylation of fucosylated digalactosylated structures with bisecting GlcNAc in total IgG glycans-FBG2S2/(FBG2 + FBG2S1 + FBG2S2) = GP24/SUM(GP24 + GP15 + GP19)* 100; ratio of all fucosylated (± bisecting GlcNAc) monosialylated and disialylated structures in total IgG glycans-$F^{total}S1/F^{total}S2$ = SUM(GP16 + GP18 + GP19)/SUM(GP23 + GP24); ratio of fucosylated (without bisecting GlcNAc) monosialylated and disialylated structures in total IgG glycans-FS1/FS2 = SUM(GP16 + GP18)/GP23; ratio of fucosylated (with bisecting GlcNAc) monosialylated and disialylated structures in total IgG glycans - FBS1/FBS2 = GP19/GP24; ratio of all fucosylated sialylated structures with and without bisecting GlcNAc-FBS^{total}/FS^{total} = SUM(GP19 + GP24)/SUM(GP16 + GP18 + GP23); ratio of fucosylated monosialylated structures with and without bisecting GlcNAc-FBS1/FS1 = GP19/SUM(GP16 + GP18); the incidence of bisecting GlcNAc in all fucosylated monosialylated structures in total IgG glycans-FBS1/(FS1 + FBS1) = GP19/SUM(GP16 + GP18 + GP19); ratio of fucosylated disialylated structures with and without bisecting GlcNAc - FBS2/FS2 = GP24/GP23; the incidence of bisecting GlcNAc in all fucosylated disialylated structures in total IgG glycans - FBS2/(FS2 + FBS2) = GP24/SUM(GP23 + GP24). The following derived traits were approximated only from the ratios of glycan peaks containing neutral glycan as a major structure. First, the percentage of each neutral glycan peak ($GP1^n$ - $GP15^n$) was calculated from the total neutral glycan fraction (SUM(GP1:GP15)) and then traits were defined as: the percentage of agalactosylated structures in total neutral glycan fraction-$G0^n$ = SUM($GP1^n$ + $GP2^n$ + $GP4^n$ + $GP6^n$); the percentage of monogalactosylated structures in total neutral glycan fraction - $G1^n$ = SUM($GP7^n$ + $GP8^n$ + $GP9^n$ + $GP10^n$ + $GP11^n$); the percentage of digalactosylated structures in total neutral glycan fraction - $G2^n$ = SUM($GP12^n$ + $GP13^n$ + $GP14^n$ + $GP15^n$); the percentage of all fucosylated (±bisecting GlcNAc) structures in total neutral glycan fraction - $F^{n\ total}$ = SUM($GP1^n$ + $GP4^n$ + $GP6^n$ + $GP8^n$ + $GP9^n$ + $GP10^n$ + $GP11^n$ + $GP14^n$ + $GP15^n$); the percentage of fucosylation of agalactosylated structures-$FG0^{n\ total}/G0^n$ = SUM($GP1^n$ + $GP4^n$ + $GP6^n$)/$G0^n$ * 100; the percentage of fucosylation of monogalactosylated structures-$FG1^{n\ total}/G1^n$ = SUM($GP8^n$ + $GP9^n$ + $GP10^n$ + $GP11^n$)/$G1^n$ * 100; the percentage of fucosylation of digalactosylated structures-$FG2^{n\ total}/G2^n$ = SUM($GP14^n$ + $GP15^n$)/$G2^n$ * 100; the percentage of fucosylated (without bisecting GlcNAc) structures in total neutral glycan fraction-F^n = SUM($GP1^n$ + $GP4^n$ + $GP8^n$ + $GP9^n$ + $GP14^n$); the percentage of fucosylation (without bisecting GlcNAc) of agalactosylated structures - $FG0^n/G0^n$ = SUM($GP1^n$ + $GP4^n$)/$G0^n$ * 100; the percentage of fucosylation (without bisecting GlcNAc) of monogalactosylated structures -$FG1^n/G1^n$ = SUM($GP8^n$ + $GP9^n$)/$G1^n$ * 100; the percentage of fucosylation (without bisecting GlcNAc) of digalactosylated structures-$FG2^n/G2^n$ = $GP14^n/G2^n$ * 100; the percentage of fucosylated (with bisecting GlcNAc) structures in total neutral glycan fraction-FB^n = SUM($GP6^n$ + $GP10^n$ + $GP11^n$ + $GP15^n$); the percentage of fucosylation (with bisecting GlcNAc) of agalactosylated structures-$FBG0^n/G0^n$ = $GP6^n/G0^n$ * 100; the percentage of fucosylation (with bisecting GlcNAc) of monogalactosylated structures-$FBG1^n/G1^n$ = SUM($GP10^n$ + $GP11^n$)/$G1^n$ * 100; the percentage of fucosylation (with bisecting GlcNAc) of digalactosylated structures-$FBG2^n/GP2^n$ = $GP15^n/G2^n$ * 100; ratio of fucosylated structures with and without bisecting GlcNAc-FB^n/F^n = FB^n/F^n; the incidence of bisecting GlcNAc in all fucosylated structures in total neutral glycan fraction-$FB^n/F^{n\ total}$ = $FB^n/F^{n\ total}$ * 100; ratio of fucosylated non-bisecting GlcNAc structures and all structures with bisecting GlcNAc-$F^n/(B^n + FB^n)$ = $F^n/(GP13^n + FB^n)$; ratio of structures with bisecting GlcNAc and all fucosylated structures (± bisecting GlcNAc)-$B^n/(F^n + FB^n)$ (‰) = $GP13^n/(F^n$+ % $FB^n)$ * 1000; ratio of

fucosylated digalactosylated structures with and without bisecting GlcNAc-FBG2^n/FG2^n = GP15^n/GP14^n; the incidence of bisecting GlcNAc in all fucosylated digalactosylated structures in total neutral glycan fraction-FBG2^n/(FG2^n + FBG2^n) = GP15^n/(GP14^n + GP15^n) × 100; ratio of fucosylated digalactosylated nonbisecting GlcNAc structures and all digalactosylated structures with bisecting GlcNAc-FG2^n/(BG2^n + FBG2^n) = GP14^n/(GP13^n + GP15^n); ratio of digalactosylated structures with bisecting GlcNAc and all fucosylated digalactosylated structures (±bisecting GlcNAc)-BG2^n/(FG2^n + FBG2^n) (‰) = GP13^n/(GP14^n + GP15^n) * 1000.

Overview of derived traits and glycans structures present in each chromatographic peak is available as supplemental Table S1.

Molecular Modeling—Molecular modeling was performed on a Silicon Graphics Fuel work station using InsightII and Discover software (MSI Inc.). The crystal structure of IgG Fc (42) was used as the basis for modeling (pdb code 1H3V; obtained from the Protein Data Bank (43). The IgG Fc used for crystallization contains A2G2F glycans at Asn 297, but the majority of the 3-arm is disordered in the crystal. Preferred conformations for the bisecting GlcNAc were obtained from the database of glycosidic linkage conformations (44, 45).

Statistical Analysis—The descriptive part of this study was based on non-parametric methods because deviations from normal distribution were observed. Correlations were performed with Spearman's rank test and gender differences were tested with the Mann-Whitney test. The basic analysis was performed in genealogy unlinked individuals, in order not to bias the results with sample relatedness. The sample size for the subset of these analyses was thus reduced to 612 samples from Vis Island (67.5% of the full sample size), 520 samples (56.8%) from Korčula Island and 477 from Orkney islands, or 1609 samples in total. SPSS version 13 was used in the analysis (SPSS Inc, Chicago, IL). In the last step of analysis we used pedigree information and entire sample size to establish relationships between respondents to calculate heritability estimates. Heritability analysis was conducted using polygenic models in Sequential Oligogenic Linkage Analysis Routines (46). Age and sex were used as predictor variables in these models. Significance was set at $p < 0.05$.

RESULTS AND DISCUSSION

Development of a New Affinity Material and Purification of IgG from 2298 Human Plasma Samples—The newly developed protein G monolithic plate with the bed volume of a single protein G column of 150 μl was used for IgG purification. Plasma samples (V = 50 μl) were diluted ten times with PBS, pH 7.4, and loaded onto the columns. The dynamic binding capacity for IgG was not exceeded. The purity of eluted fractions was examined by SDS-PAGE revealing two clearly visible bands corresponding to the molecular masses of heavy (~50 kDa) and light chains (~25 kDa) of IgG (supplemental Fig. S1).

The newly developed 96-well protein G plates were used to purify IgG from 2298 plasma samples. The entire chromatographic procedure for 96 samples, including the binding, washing and elution steps, was performed in less than 30 min. The concentration of IgG in human plasma varies between 6.6 and 14.5 mg/ml (47). The average amount of IgG isolated from 50 μl of plasma with the use of 96-well protein G monolithic plates was 640 μg, indicating that the majority of IgG in the sample was successfully captured and released.

Because the elution of IgG from protein G requires very low pH, there is a certain risk of loss of sialic acids because of acid hydrolysis. Isolation with monoliths minimized this risk as elution occurs within seconds and therefore the pH was quickly restored to neutrality preserving the integrity and activity of the IgG molecules. The use of a vacuum for liquid transfer enabled easy and efficient handling of large sample sets.

Analysis of IgG Glycans—*N*-glycans attached to IgG were released using PNGase F and labeled with 2-aminobenzamide (2-AB). Labeled glycans were separated by hydrophilic interaction chromatography on a recently introduced Waters BEH Glycan chromatography column. Because this was the first application of this column for the analysis of IgG glycans in our laboratory, each chromatographic peak was collected and analyzed by exoglycosidase digestion (data not shown) and mass spectrometry to determine the glycan structures that elute in each peak (supplemental Table S2). A total of 23 major and 10 minor glycan structures were successfully resolved (Fig. 1, Table I). An additional 40 glycosylation traits (galactosylation, core fucosylation, sialylation, etc.) were derived from ratios of these glycan peaks as described in the *Experimental Procedures* section.

Approximately 96% of all neutral IgG glycans contained core fucose (Table II: F$^{n\ \mathrm{total}}$). In contrast with immunoglobulins, which are mainly produced by B-cells, other major plasma glycoproteins generally originate from hepatocytes, which express only very low levels of the FUT8 fucosyltransferase and thus contain a low percentage of core fucosylated glycans (48). They are also generally more highly sialylated and consequently over 35% of all glycans in human plasma are A2G2S2 structures (38). The median level of A2G2S2 glycans in our IgG preparations was slightly over 3% (Table II: GP21), which is very similar to previously reported values (49). This indicated that the level of contaminating plasma proteins in our IgG preparations was very low, but because disialylated structures without core fucose on IgG are of rather low frequency, even low level of contaminating plasma proteins would cause significant errors in calculation of the sialylation level. To minimize this problem, all calculations of sialylation-related traits were performed using only core fucosylated structures, which are predominant on IgG and less abundant on other plasma proteins.

Galactosylation—Galactosylation of IgG is one of the most studied glycosylation feature of any glycoprotein. Because the discovery of decreased galactosylation of IgG in rheumatoid arthritis more than 25 years ago (10), over 50 different studies have analyzed the role of IgG galactosylation in different inflammatory diseases (50). In our three populations, neutral glycans without galactoses (G0^n) were slightly below 40%, neutral glycans with one terminal galactose (G1^n) slightly above 40% and neutral glycans with two terminal galactoses (G2^n) were ~20% of the neutral IgG glycome (Table II). Because only 11.6% of G1 was sialylated (Table II:

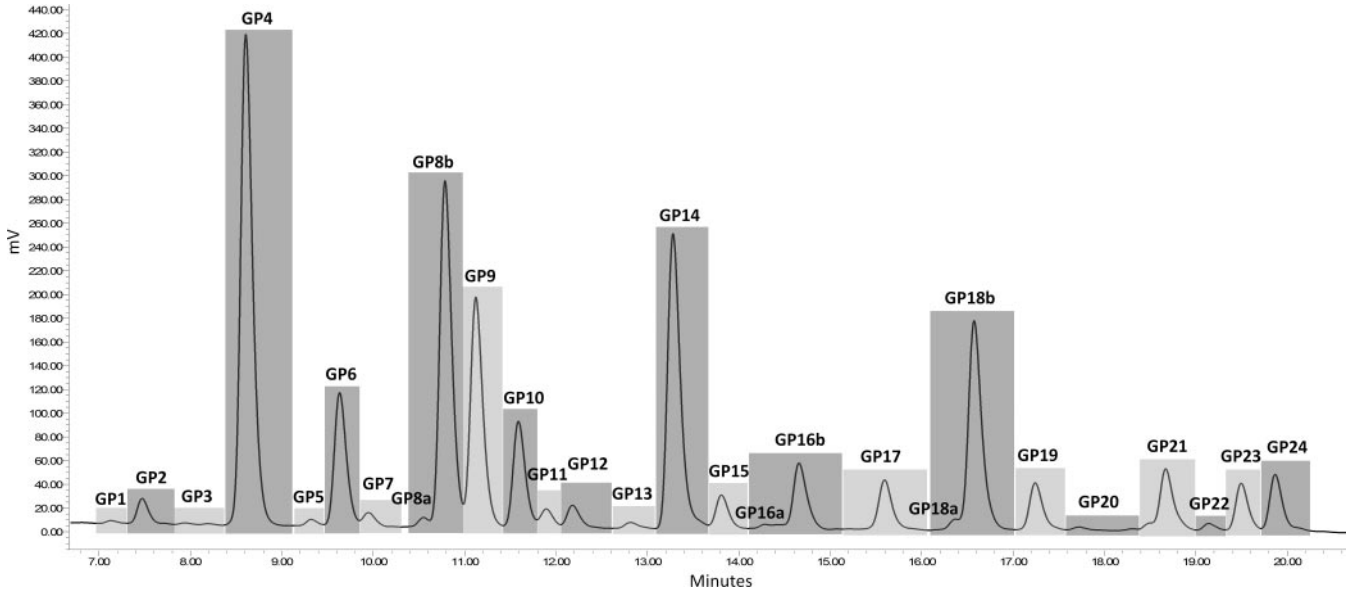

FIG. 1. **UPLC analysis of the IgG glycome.** IgG glycome was separated into 24 chromatographic peaks by hydrophilic interaction chromatography. Compositions and structural schemes of glycans in each chromatographic peak and the average percentage of individual structures are shown in Table I.

FG1S1/(FG1+FG1S1)), whereas over 50% of G2 was sialylated (Table II: FG2S2/(FG2+FG2S1+FG2S2) and FBG2S2/(FBG2+FBG2S1+FBG2S2)), in the total pool of IgG glycans, median levels of a galactosylated, mono galactosylated, and digalactosylated structures-the latter two with or without sialic acid-were approximately the same. However, the ratio of G0^n to G2^n increased significantly with age, (see section "*Effects of Gender and Age*"), thus the observed equilibrium between glycans with different number of galactoses could be a peculiarity of our relatively old study cohorts.

A clear preference for the addition of the first galactose to the antennae, which extend from the α1–6 linked mannose residues of the trimannosyl core (6-arm), was observed because over 65% of G1^n structures contained galactose on the 6-arm (Table II: GP8/(GP8+GP9)). This difference was even larger in structures containing bisecting GlcNAc where over 85% of all G1^n structures contained galactose on the 6-arm (Table II: GP10/(GP10+GP11)). This is in accordance with previous studies, which demonstrated that on native IgG it is the 6-arm, which is preferentially galactosylated (51), despite the fact that galactosyltransferase preferentially galactosylates the 3-arm of free biantennary glycans *in vitro* (52). This apparent paradox results from the fact that glycans attached to Asn_{297} of IgG are located in a cleft between the two heavy chains (53), which affects their accessibility to glycosyltransferases. Oligosaccharides and the polypeptide chains of the C_H2 domain form multiple noncovalent bonds (54). The majority of these interactions occur between the elongated antennae that extend from the α1–6 linked mannose residues of the trimannosyl cores whereas the 3-arm extends into the interstitial space between the C_H2 domains and is therefore less accessible to glycosyltransferases (42). Moreover, the addition of a galactose to the 3-arm does not directly affect the accessibility of the 6-arm allowing the G1 glycan to be converted to G2, whereas the addition of galactose to the 6-arm reduces accessibility of the 3-arm and prevents further processing (55).

Sialylation—Sialylation of IgG recently attracted much attention after it was shown that it is responsible for the anti-inflammatory activity of intravenously administered immunoglobulins (11, 56). IgG antibodies have long been recognized as proinflammatory mediators of the humoral immune response. Appropriate glycosylation of Asn_{297} is essential for the proinflammatory activity of IgG antibodies by maintaining the heavy chains in conformation, which favors binding to Fcγ receptors (57). Enzymatic removal of this glycan significantly reduces FcγR binding and, consequently, the proinflammatory activity *in vivo* (58). However, if the glycan is sialylated, the proinflammatory effect of IgG is reversed and it now exerts anti-inflammatory effects (56), most probably through interactions with the lectin receptor SIGN-R1 or DC-SIGN (12). This has significant implications for both the normal function of IgG in the immune response and the application of intravenous immunoglobulins for the treatment of a number of autoimmune diseases (59).

Approximately 10% of IgG glycans were found to terminate in sialic acid in a number of early studies (57). We found that in our population the percentage of sialylated glycans was significantly higher with median values being ~20% in core fucosylated glycans without bisecting GlcNAc (Table II: FGS/(F+FG+FGS)) and 29.5% in core fucosylated glycans with bisecting GlcNAc (Table II: FBGS/(FB+FBG+FBGS)). The most probable cause for this apparent difference is the improvement in methodology, which results in decreased hy-

TABLE I

Composition of the IgG glycome. IgG glycome was separated into 24 chromatographic peaks by hydrophilic interaction chromatography. Structures of glycans in each chromatographic peak and the average percentage of individual structures (%) were determined by mass spectrometry. Structure abbreviations: all N-glycans have core sugar sequence consisting of two N-acetylglucosamines (GlcNAc) and three mannose residues; F indicates a core fucose α1–6 linked to the inner GlcNAc; Mx, number (×) of mannose on core GlcNAcs; Ax, number of antenna (GlcNAc) on trimannosyl core; A2, biantennary glycan with both GlcNAcs as β1–2 linked; B, bisecting GlcNAc linked β1–4 to β1–3 mannose; Gx, number of β1–4 linked galactose (G) on antenna; [3]G1 and [6]G1 indicates that the galactose is on the antenna of the α1–3 or α1–6 mannose; Sx, number (×) of sialic acids linked to galactose. Structural schemes are given in terms of N-acetylglucosamine (square), mannose (circle), fucose (rhomb with a dot), galactose (rhomb) and sialic acid (star)

Glycan peak	Peak composition	Structure	%
GP1	F(6)A1		100
GP2	A2		100
GP3	A2B		100
GP4	F(6)A2		100
GP5	M5		63
	F(6)A2		37
GP6	F(6)A2B		97
	A2[6]G1		3
GP7	A2[3]G1		75
	F(6)A2B		25
GP8a	A2BG1		93
	F(6)A2[6]G1		7
GP8b	F(6)A2[6]G1		100
GP9	F(6)A2[3]G1		100
GP10	F(6)A2[6]BG1		100
GP11	F(6)A2[3]BG1		100
GP12	A2G2		91
	F(6)A2[3]BG1		9
GP13	A2BG2		87
	F(6)A2G2		13
GP14	F(6)A2G2		100

Glycan peak	Peak composition	Structure	%
GP15	F(6)A2BG2		83
	F(6)A1G1S1	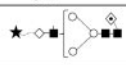	8
	A2G1S1	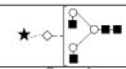	5
	F(6)A2G2		4
GP16a	F(6)A2[6]G1S1	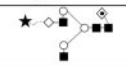	63
	M4A1G1S1	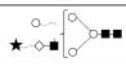	25
	A2BG1S1	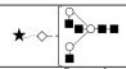	13
GP16b	F(6)A2[3]G1S1	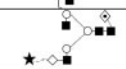	91
	F(6)A2[6]BG1S1	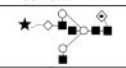	9
GP17	A2G2S1	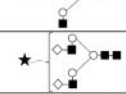	89
	F(6)A2[3]BG1S1	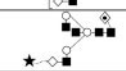	11
GP18a	A2BG2S1	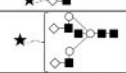	91
	F(6)A2G2S1	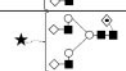	9
GP18b	F(6)A2G2S1	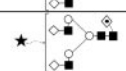	100
GP19	F(6)A2BG2S1	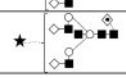	100
GP20	n.d.		/
GP21	A2G2S2	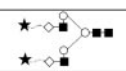	100
GP22	A2BG2S2	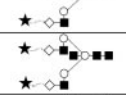	100
GP23	F(6)A2G2S2	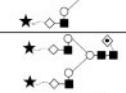	100
GP24	F(6)A2BG2S2		100

TABLE II

Descriptives of the IgG glycome in three populations. IgG glycans were analyzed for individuals from the Croatian Adriatic islands Vis (n = 915), Korčula (n = 906) and Orkney (n = 477). Median values, interquartile ranges (IQR), and minimal and maximal values are shown. Calculations and descriptions of derived glycosylation traits are explained in the Experimental Procedures section. An extended list of derived glycan features is available in supplementary Table S3

IgG glycan	Population: Vis		Population: Korčula		Population: Orkney	
	Median (IQR)	Min-Max	Median (IQR)	Min-Max	Median (IQR)	Min-Max
GP1	0.16 (0.19)	0.02–2.38	0.15 (0.12)	0.03–1.02	0.16 (0.1)	0.04–1.24
GP2	0.74 (0.55)	0.11–5.2	0.72 (0.57)	0.14–9.39	0.71 (0.53)	0.17–4.59
GP4	20.39 (8.61)	6.56–42.37	20.05 (8.54)	6.07–41.34	20.14 (8.17)	8.08–49.47
GP5	0.31 (0.13)	0.09–0.97	0.29 (0.14)	0.12–0.97	0.27 (0.09)	0.13–0.84
GP6	5.24 (2.15)	1.93–12.86	5.5 (2.2)	1.79–11.09	4.82 (2.11)	1.95–10.65
GP7	0.67 (0.52)	0.14–4.01	0.68 (0.46)	0.15–4.06	0.48 (0.31)	0.12–1.72
GP8	16.42 (2.61)	9.84–23.7	16.2 (2.53)	8.93–23.56	18.08 (2.21)	11.89–25.4
GP9	7.9 (1.57)	4.27–11.8	7.95 (1.69)	4.6–12.19	8.98 (1.59)	5.01–12.5
GP10	4.59 (1.3)	2.48–10.2	4.6 (1.22)	2.59–8.19	4.48 (1.11)	2.64–13.37
GP11	0.75 (0.2)	0.33–2.92	0.76 (0.2)	0.4–1.82	0.77 (0.19)	0.44–1.41
GP12	0.96 (0.64)	0.26–6.14	0.98 (0.69)	0.23–3.91	0.8 (0.5)	0.21–3.87
GP13	0.25 (0.16)	0.08–1.59	0.22 (0.07)	0.1–1.01	0.24 (0.07)	0.13–0.58
GP14	11.02 (5.06)	3.39–22.97	10.77 (4.83)	3.5–24.81	12.26 (5.07)	3.66–23.91
GP15	1.41 (0.48)	0.71–2.89	1.51 (0.46)	0.68–2.81	1.64 (0.45)	0.77–2.83
GP16	3.13 (0.68)	1.99–5.11	3.21 (0.61)	1.82–5.22	3.21 (0.61)	1.69–5.25
GP17	2.61 (1.85)	1–13.61	2.43 (1.67)	0.94–10.45	1.58 (0.53)	0.92–7.73
GP18	8.58 (3.65)	3.96–18.02	8.83 (3.52)	3.58–26.02	9.33 (3.67)	3.45–18.92
GP19	2.45 (0.7)	1.16–9.03	2.41 (0.63)	1.15–5.1	2.38 (0.48)	1.3–4.54
GP20	0.43 (0.43)	0.07–3.25	0.62 (0.49)	0.11–3.46	0.49 (0.22)	0.25–2.56
GP21	3.41 (2.38)	1.03–23.82	3.2 (2.83)	0.98–24.6	1.56 (0.68)	0.67–6.01
GP22	0.36 (0.21)	0.06–1.33	0.31 (0.13)	0.08–1.46	0.29 (0.12)	0.06–0.88
GP23	1.98 (0.79)	0.71–13.73	2.27 (0.83)	0.9–4.67	2.3 (0.89)	0.88–4.62
GP24	2.7 (0.79)	1.02–7.66	2.72 (0.78)	0.67–5.84	2.66 (0.71)	0.97–8.86
FGS/(FG+FGS)	28.15 (4.52)	17.59–47.45	29.5 (4.54)	19.02–42.8	27.32 (4.09)	19.63–37.27
FBGS/(FBG+FBGS)	43.14 (8.86)	14.07–74.67	43.05 (7.84)	21.95–60.72	41.96 (7.16)	12.06–66.91
FGS/(F+FG+FGS)	19.71 (6.03)	9.67–42.34	20.82 (5.82)	9.63–39.62	19.99 (5.39)	9.14–32.28
FBGS/(FB+FBG+FBGS)	29.91 (7.99)	10.16–65.45	29.38 (7.64)	14.17–48.83	29.70 (7.36)	10.37–51.19
FG1S1/(FG1+FG1S1)	11.49 (2.59)	7.38–22.13	11.79 (2.33)	7.21–22.05	10.67 (2.02)	5.99–15.84
FG2S1/(FG2+FG2S1+FG2S2)	39.99 (3.28)	32.05–49.45	40.72 (3.22)	33.24–50.07	39.16 (3.26)	25.21–48.48
FG2S2/(FG2+FG2S1+FG2S2)	8.99 (3.3)	3.61–33.21	10.08 (3.44)	2.18–30.64	9.45 (2.79)	4.18–20.31
FBG2S1/(FBG2+FBG2S1+FBG2S2)	37.2 (4.73)	26.27–49.34	36.2 (4.66)	25.86–46.49	35.92 (4)	26.32–44.75
FBG2S2/(FBG2+FBG2S1+FBG2S2)	41.09 (5.92)	23.09–59.58	40.73 (5.77)	15.88–54.25	39.48 (4.59)	18.91–62.28
FBS1/(FS1+FBS1)	0.17 (0.05)	0.08–0.52	0.17 (0.05)	0.04–0.36	0.16 (0.05)	0.07–0.31
FBS2/(FS2+FBS2)	0.58 (0.08)	0.36–0.75	0.55 (0.08)	0.37–0.78	0.54 (0.08)	0.32–0.78
$G0^n$	37.09 (12.75)	14.69–69.57	37.22 (11.66)	13.84–62.82	34.62 (11.46)	16.17–69.42
$G1^n$	42.6 (4.54)	24.18–50.96	42.73 (4.38)	29.59–49.26	44.45 (3.78)	24.73–60.27
$G2^n$	19.17 (8.83)	5.93–43.76	18.88 (8.24)	7.05–47.09	20 (8.47)	5.64–40.27
$F^{n\ total}$	95.77 (2.32)	84.19–98.64	95.76 (2.37)	80.7–98.64	96.52 (1.8)	88.16–98.67
$FG0^{n\ total}/G0^n$	97.11 (1.95)	81.33–99.59	97.26 (2.09)	77.55–99.52	97.15 (1.89)	86.42–99.41
$FG1^{n\ total}/G1^n$	97.78 (1.67)	87.05–99.57	97.76 (1.57)	86.77–99.54	98.52 (0.91)	94.55–99.6
$FG2^{n\ total}/G2^n$	91.03 (5.05)	72.7–97.35	90.88 (4.32)	73.66–98.08	92.95 (3.37)	80.66–97.51
F^n	78.3 (4.62)	63.83–87.48	77.99 (4.72)	60.95–86.52	80.44 (4.05)	67.55–88.92
$FG0^n/G0^n$	77.02 (5.22)	49.91–86.55	76.18 (5.93)	53.13–86.54	78.3 (5.24)	59.25–88.33
$FG1^n/G1^n$	79.5 (4.5)	66.38–87.63	79.68 (4.46)	67.99–87.69	82.28 (4.1)	68.72–90.2
$FG2^n/G2^n$	80.42 (5.74)	57.71–90.2	79.48 (5.58)	60.13–89.57	81.59 (5.28)	63.28–90.49
FB^n	16.92 (3.45)	10.87–25.9	17.27 (3.61)	10.49–26.43	15.74 (3.37)	9–26.36
$FBG0^n/G0^n$	19.85 (4.57)	12.16–33.2	20.64 (4.7)	11.66–36.83	18.74 (4.14)	10.51–32.08
$FBG1^n/G1^n$	17.78 (3.91)	11.1–28.42	17.74 (4)	10.73–28.46	16.17 (4.07)	8.85–30.76
$FBG2^n/G2^n$	10.27 (2.39)	6.36–30.92	11.13 (3.06)	5.78–24.33	10.95 (3.06)	5.72–20.94
$FB^n/F^{n\ total}$	17.76 (3.72)	11.05–27.64	18.18 (3.94)	10.85–27.81	16.35 (3.51)	9.23–26.91

drolysis of sialic acids during the purification of IgG and glycan analysis. Both rapid elution and neutralization enabled by the use of newly developed protein G monolithic plates, and the replacement of hydrazide (used in early studies) with PNGase F contributed to the better preservation of sialic acid. However, it should be noted that some previous studies analyzed only heavy chains of IgG, thus the Fab light chain glycans (which are generally more sialylated) bound to light chains of IgG were excluded from the analysis. In addition, a recent interlaboratory comparison of glycan analysis methods revealed that mass spectrometry routinely underestimated sialic acid on IgG by nearly 3-fold, whereas HPLC analysis reported sialylation levels very similar to the sialylation levels observed in our populations (60). However, this interlaboratory comparison was performed on a small number of samples, and our study is the first large scale study to reported

TABLE III

Heritability of the IgG glycome. Heritability of individual glycans in the population of the Croatian Adriatic island Vis was estimated using polygenic models in Sequential Oligogenic Linkage Analysis Routines (SOLAR)

IgG glycan	Covariates significance					
	H2	P (H2)	S.E. (H2)	Gender	Age	R^{2a}
GP1	26.8%	0.010	0.117	0.771	2.00E-02	0.7%
GP2	26.1%	0.023	0.134	0.411	6.63E-24	11.1%
GP4	16.9%	0.061	0.114	0.128	2.52E-81	33.7%
GP5	0.0%	0.500	-	0.001	5.66E-01	1.3%
GP6	32.8%	0.001	0.113	0.218	4.68E-66	28.0%
GP7	13.0%	0.128	0.118	0.017	2.14E-01	0.7%
GP8	29.7%	0.005	0.116	0.271	2.60E-10	4.7%
GP9	29.1%	0.009	0.127	0.007	2.36E-01	1.0%
GP10	43.3%	0.000	0.118	0.037	2.18E-01	0.5%
GP11	17.0%	0.080	0.126	0.009	1.12E-14	7.2%
GP12	10.9%	0.170	0.118	0.049	3.65E-12	5.6%
GP13	1.5%	0.445	0.108	0.383	3.30E-02	0.6%
GP14	44.5%	0.000	0.112	0.040	4.85E-72	30.5%
GP15	36.2%	0.007	0.113	0.001	1.62E-30	14.9%
GP16	29.8%	0.008	0.127	0.074	7.30E-02	0.7%
GP17	27.9%	0.003	0.105	0.005	7.50E-02	1.2%
GP18	47.8%	0.000	0.112	0.329	7.86E-61	26.3%
GP19	40.3%	0.000	0.123	0.000	6.00E-02	2.2%
GP20	0.0%	0.500	-	0.001	8.46E-01	1.3%
GP21	19.3%	0.055	0.124	0.004	8.90E-03	1.8%
GP22	0.0%	0.500	-	0.309	6.12E-01	0.1%
GP23	17.9%	0.063	0.121	0.996	3.03E-11	4.8%
GP24	46.0%	0.000	0.113	0.008	1.22E-01	1.1%
FGS/(FG+FGS)	19.8%	0.052	0.126	0.099	7.74E-09	4.0%
FBGS/(FBG+FBGS)	39.7%	0.002	0.131	0.079	5.00E-03	1.4%
FGS/(F+FG+FGS)	21.7%	0.027	0.117	0.503	5.14E-58	25.4%
FBGS/(FB+FBG+FBGS)	11.5%	0.183	0.129	0.376	1.17E-07	3.2%
FG1S1/(FG1+FG1S1)	14.4%	0.118	0.123	0.740	1.75E-06	2.5%
FG2S1/(FG2+FG2S1+FG2S2)	40.2%	0.002	0.134	0.107	2.29E-02	0.8%
FG2S2/(FG2+FG2S1+FG2S2)	42.4%	0.000	0.121	0.443	2.03E-23	10.4%
FBG2S1/(FBG2+FBG2S1+FBG2S2)	47.9%	0.000	0.129	0.022	4.24E-19	9.3%
FBG2S2/(FBG2+FBG2S1+FBG2S2)	61.3%	0.000	0.110	0.810	2.30E-11	4.9%
FBS1/(FS1+FBS1)	56.4%	0.000	0.119	0.000	1.31E-47	22.1%
FBS2/(FS2+FBS2)	42.5%	0.000	0.122	0.000	5.64E-28	13.9%
$G0^n$	35.0%	0.001	0.118	0.779	2.96E-88	35.7%
$G1^n$	26.7%	0.014	0.124	0.948	7.74E-29	13.1%
$G2^n$	42.0%	0.000	0.109	0.009	1.02E-70	30.2%
$F^{n\ total}$	37.0%	0.001	0.118	0.595	2.00E-01	0.1%
$FG0^{n\ total}/G0^n$	47.2%	0.000	0.115	0.530	8.19E-01	0.1%
$FG1^{n\ total}/G1^n$	32.0%	0.004	0.123	0.726	4.39E-01	0.1%
$FG2^{n\ total}/G2^n$	29.6%	0.005	0.116	0.814	1.93E-07	3.2%
F^n	45.4%	0.000	0.115	0.129	9.00E-05	2.3%
$FG0^n/G0^n$	45.4%	0.001	0.115	0.162	2.15E-01	0.3%
$FG1^n/G1^n$	43.1%	0.000	0.124	0.006	3.00E-04	2.8%
$FG2^n/G2^n$	13.6%	0.122	0.120	0.268	2.76E-23	10.7%
FB^n	33.3%	0.002	0.118	0.001	6.44E-18	8.8%
$FBG0^n/G0^n$	29.8%	0.008	0.126	0.000	3.15E-01	1.6%
$FBG1^n/G1^n$	32.5%	0.003	0.124	0.000	1.25E-07	4.7%
$FBG2^n/G2^n$	47.3%	0.000	0.123	0.001	1.83E-01	1.3%
$FB^n/F^{n\ total}$	29.6%	0.006	0.120	0.000	1.84E-16	8.4%

[a] Percent of variance explained in the model.

such a high level of IgG sialylation. A more extensive international interlaboratory study of glycan quantification concluded that permethylation of glycans can enable reliable quantification of sialic acid on transferrin and IgG (61).

The variability of sialylation (of galactosylated glycans) in the population was also found to be rather high, ranging from 17.6% to 47.5% in IgG without bisecting GlcNAc (Table II: FGS/(FG+FGS)), and between 12.1% and 74.7% in IgG with bisecting GlcNAc (Table II: FBGS/(FBG+FBGS)). Because our study participants came from a cross section study, it was not possible to clearly identify whether high sialylation in some individuals was a genetic predisposition or a temporary physiological condition. However, the extent of sialylation was found to be the most heritable element of IgG glycosylation (Table III) indicating strong genetic regulation. This was further supported by relatively small changes in sialylation observed in several individuals that were sampled a second time, after a period of ~12 months (supplemental Fig. S2).

The majority of IgG glycans are attached to Asn_{297} in the constant region of the heavy chain, but 15–20% of IgG also contain glycans on the variable regions and some studies indicated that these glycans are more sialylated, and particularly more bisialylated than Fc glycans (49, 62, 63). The most comprehensive comparison of Fc and Fab IgG glycans was unfortunately performed on only two control individuals and the difference of Fc sialylation in these two patients was rather large (49). However, in one of them over 70% of bigalactosylated glycans with both core fucose and bisecting GlcNAc were sialylated, what is in line with our observations. Whether the observed variability of IgG sialylation originates from Fab or Fc glycans is not known, but because individual differences in Fc sialylation could have strong effects on the inflammatory response, this issue should be addressed in future studies.

Fucosylation—Core fucosylation of IgG has been intensively studied because of its role in ADCC. Natural killer cells have receptors for the Fc domain of IgG. They bind to the Fc portion of IgG antibodies on the surface of target cells, such as tumor cells, and release cytolytic components that kill the target cell. This mechanism of killing is considered to be the major mechanism of antibody-based therapeutics against tumors. Core fucose is very important in this process because IgG deficient in core fucose on the Fc glycan was found to have ADCC activity enhanced by up to 100-fold (64). Endogenous serum IgG inhibits therapeutic antibody-induced ADCC by competing for FcγRIIIa binding sites (17), but nonfucosylated therapeutic IgG was reported to be able to evade this through higher affinity FcγRIIIa binding (16). However, this might be highly dependent on the extent of core fucosylation of host IgGs. In our populations the fraction of neutral IgG glycans without the core fucose was found to vary between 1.3% and 19.3% (Table II; $F^{n\ total}$) and this large variability could affect the efficacy of therapeutic antibodies. Individuals with lower core fucose might need higher doses of the drug, thus the extent of host IgG core fucosylation may need to be one of the parameters in the calculation of the exact therapeutic dose.

Bisecting GlcNAc—The addition of bisecting GlcNAc to the IgG glycan by GlcNAc transferase III (GnTIII) significantly affects its accessibility to other glycosyltransferases. For example, the addition of bisecting GlcNAc prevents further branching because glycans with bisecting GlcNAc are not a substrate for GnTs IV, V, and VI (65). Some studies also indicate that the presence of bisecting GlcNAc diminishes galactosylation by GalT (66) and the addition of core fucose (67).

In our study, on average, ~18% of neutral glycans contained bisecting GlcNAc (Table II: $FB^n/F^{n\ total}$). However, when the percentages of bisecting GlcNAc in $G0^n$, $G1^n$, and $G2^n$ structures were compared, a significant decrease in the percentage of bisecting GlcNAc (nearly 50%) in $G2^n$ structures was observed (Table II: $FBG0^n/G0^n$, $FBG1^n/G1^n$, and $FBG2^n/G2^n$). At first sight, this seemed to confirm the results of transfection assays, which indicated that GnTIII and GalT compete for an agalactosyl nonbisected biantennary sugar chain as a common substrate (66). However, after considering this in the context of not only neutral, but also sialylated glycans, the presence of a bisecting GlcNAc did not seem to have a significant effect on IgG galactosylation. As presented in Table II and discussed in the "sialylation" section, whereas only slightly below 10% of FA2G2 structures contained two sialic acids, over 40% of FA2BG2 structures contained two sialic acids. Consequently, the decrease in bisecting GlcNAc in neutral bigalactosylated structures (from 18% in mono galactosylated to 11% in digalactosylated) was compensated by the increase in bisecting GlcNAc in bisialylated digalactosylated glycans (from 17% in mono sialylated to over 55% in disialylated digalactosylated glycans). Therefore, the percentage of digalactosylated structures with bisecting GlcNAc was approximately the same as for agalactosylated, and monogalactosylated structures. The presence of bisecting GlcNAc apparently associated with the increased addition of a second sialic acid, and consequently bisecting GlcNAc was underrepresented in neutral digalactosylated and overrepresented in sialylated digalactosylated glycan pools.

Interactions Between Different Functional Elements of IgG Glycosylation—Mutual interactions of the four above described functional elements of IgG glycosylation have been addressed in the past, but different experimental approaches (transfections, enzymatic assays, etc) often yielded conflicting results. Our study is the first large-scale detailed analysis of IgG glycosylation in well-characterized human populations, which has therefore enabled reliable conclusions about the interrelation of different functional elements. However, it is important to note that *in vivo* differences in the ratios of different glycosylation elements in IgG may not simply reflect the kinetic characteristics of relevant glycosyltransferases, but may result from regulatory elements, which govern IgG glycosylation and modulate their glycans, presumably according to the prevailing functional needs of the host organism. Only the most interesting associations are presented below, whereas the complete set of correlation coefficients and their p values is available as supplemental material (supplemental Table S4).

Recently we reported the existence of a negative correlation between galactosylation and sialylation in the human plasma glycome (68 + unpublished observations). A similar association was also found in the IgG glycome where the percentage of bigalactosylated structures in the neutral IgG glycome strongly negatively correlated with the percentage of disialylated glycans ($r = -0.39$, $p = 7.3E\text{-}43$; supplemental Fig. S3). One interpretation of this observation is that sialylation might be a rate-limiting step and that smaller amount of bigalactosylated structures can be more efficiently sialylated. The same observation could also be a reflection of the simple fact that bigalactosylated glycan is a substrate for sialyl-transferase and that efficient sialylation is decreasing

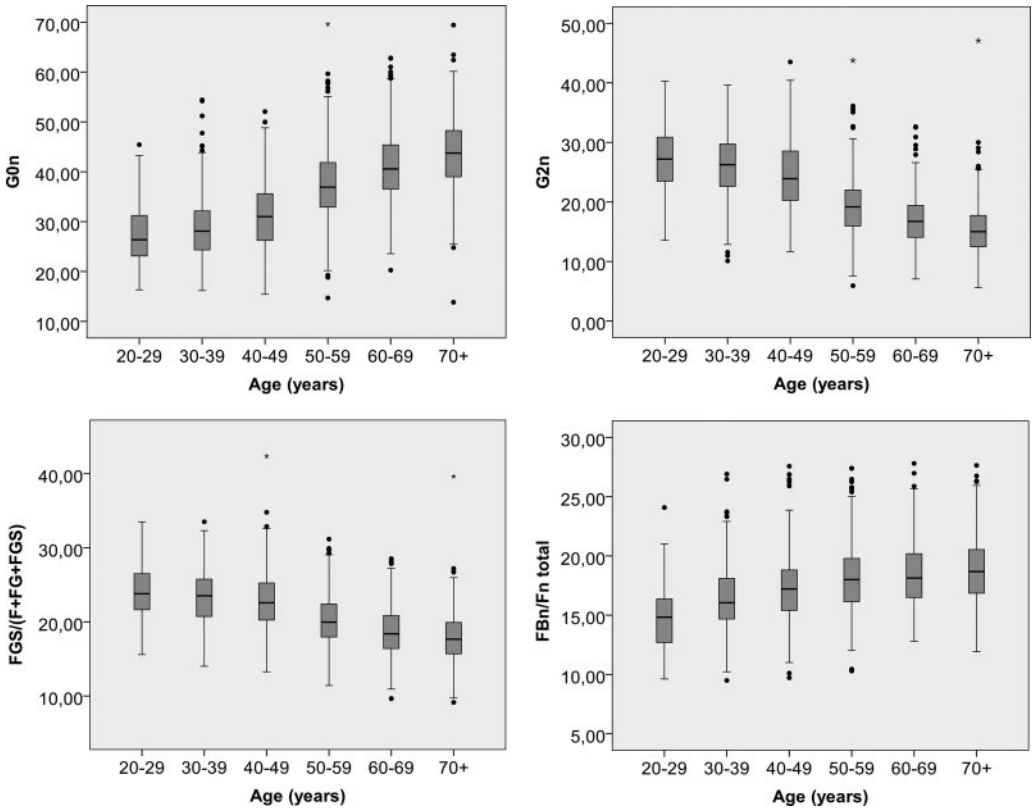

FIG. 2. **Association of IgG glycosylation with age.** Distribution of G0^n glycans, G2^n glycans, the percent of structures with sialic acid (FGS/(F+FG+FGS)) and bisecting GlcNAc (FB^n/F$^{n\ total}$) in fucosylated glycans between different age-groups are shown. Central box represents the values from the lower to upper quartile (25 to 75 percentile). The middle line represents the median. The horizontal line extends from the minimum to the maximum value, excluding "outside" and "far out" values that are displayed as separate points.

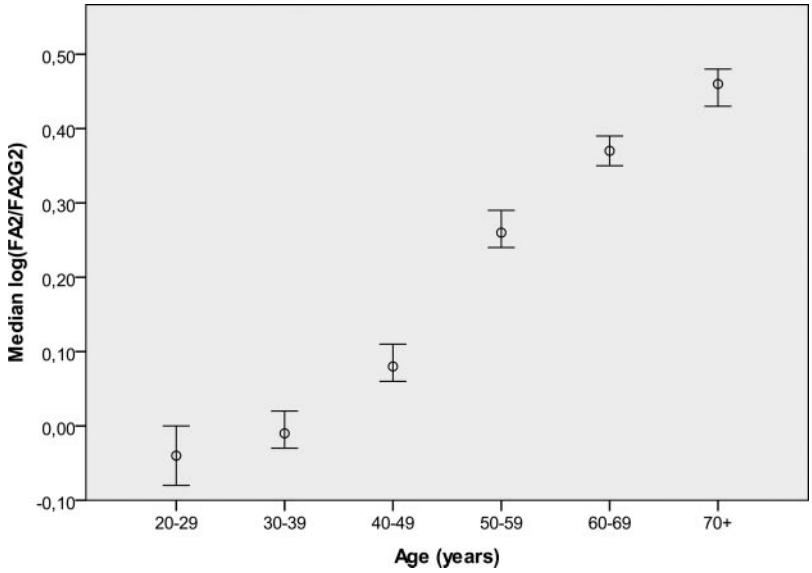

FIG. 3. **The Glyco-Age index.** Glyco-Age index calculated as the logarithm of the ratio of fucosylated G2 and G0 structures (FA2/FA2G2) was recently suggested to be a good indicator of individual's age (78). Median values of the Glyco-Age index (with 95% confidence intervals as error bars) in our study population are shown.

the level of bigalactosylated glycans in the neutral glycome by converting them into charged monosialylated and disialylated digalactosylated glycans. However, in that case monosialylated glycans should also negatively correlate with the percentage of digalactosylated glycans, what was not the case (supplemental Table S4).

Bisecting GlcNAc was reported to negatively affect both galactosylation (66) and fucosylation of IgG (67). A moderate negative ($r = -0.27$), but statistically highly significant ($p = 1.75E-20$) correlation was observed between bisecting GlcNAc (FB^n/F^n total) and core fucosylation of IgG (F^n total), which confirmed the results from *in vitro* studies. However, in our study we did not observe any negative correlation between the percentage of bisecting GlcNAc and galactosylation, indicating that *in vivo* there is no competition between GnTIII and GalT. GnTIII, which adds bisecting GlcNAc, and GalT, which adds galactoses clearly compete for the same substrate (66). The fact that this is not happening *in vivo* is a very important observation because it demonstrates that final glycan structures are not a simple result of competing enzymatic activities, but a predesigned outcome, presumably fitted to the needs of the producing cells by some still unknown regulatory mechanisms. Confirmation of this interpretation was provided by the comparison of Fab and Fc glycans in different myeloma lines, which revealed strong site-specific regulation of glycosylation (69).

The most surprising observation was the large increase in the proportion of bisecting GlcNAc in disialylated structures (FA2BG2S2, GP24), or alternatively the increase in sialylation of FA2BG2 glycans. Although ~18% of all IgG Glycans (Table II: $FB^n/F^{n\ total}$) contained bisecting GlcNAc, over 58% of all disialylated glycans contained bisecting GlcNAc (supplemental Table S3: FBS2/(FBS+FBS2). Because FA2BG2S2 structure (GP24) represents only 2.7% of the total glycome, an additional check was performed to confirm that this structure did not originate from contaminating plasma proteins. In the total serum glycome, the ratio of A2G2S2 and FA2BG2S2 structures is ~50:1 (70). Because the median value of A2G2S2 (GP21) in our population was 3.3, even if all of it originated from contaminating plasma proteins, the amount of FA2BG2S2 coming from the plasma proteins could be only up to 0.06%, which is far below the level that could significantly contribute to the observed increase in the proportion of bisecting GlcNAc in disialylated IgG glycans.

Molecular modeling of IgG Fc with a bisecting GlcNAc on the Asn 297 glycan shows that the bisect can be accommodated in a low energy linkage conformation with the rest of the glycan remaining in its crystallographic position (*i.e.* with the 6-arm bound to the surface of the protein). However, the N-acetyl group of the bisect is oriented close to the 6-arm GlcNAc and Phe 243 and may alter or disrupt the hydrophobic stacking between these two residues. This could result in the glycan 6-arm interacting less strongly with the protein surface, making the entire glycan more mobile and both 3- and 6-arms more likely to be available to glycosyltransferases.

Variability and Heritability of IgG Glycosylation—In our recent analysis of the total plasma glycome in 915 individuals from the Croatian island of Vis we observed a median ratio of minimal to maximal values of 6.17 and significant age- and gender-specific differences (38). This study (which also includes the Vis cohort) analyzed only the IgG glycome and revealed even higher variability in the population with median ratio of minimal to maximal values of 17.2 for the whole IgG glycome and 19.7 for the neutral IgG glycome. The variability of neutral glycans primarily originated from various percentage of bisecting GlcNAc and core fucose on different neutral structures that represent a relatively small part of the glycome, but even in some main glycosylation features the variability was rather high. For example the proportion of G0 ranged between 14 and 70% and the proportion of G2 between 6 and 47% (Table II). Bisecting GlcNAc and core fucose also varied significantly, but the most variable was the sialylation of different glycan structures. The disialylated form of FA2G2 varied between 2.2 and 33% (Table II: FG2S2/(FG2+FG2S1+FG2S2)), whereas the disialylated form of FA2BG2 varied between 16 and 60% (Table II: FBG2S2/(FBG2+FBG2S1+FBG2S2)).

Variations observed in a human phenotype are generally a combination of genetic differences and environmental factors. Heritability is one of the most basic and often one of the first analyses to be made in a genetic study, because it represents the proportion of the trait variance that can be attributed to genetic factors, and it is often used as a screening tool to determine whether a trait may be suitable for gene mapping (71). The fact that there are hundreds of genes involved in the complex glycan metabolic pathways argues in favor of a strong genetic influence, but environmental effects on glycan structures have also been reported (72–75). Recently we reported that there is a broad range of variation in heritability levels of plasma glycans, from insignificant or very low to over 50% for some glycans (38).

Using the large number of known genealogical relationships in our isolated populations we were able to reliably estimate heritability of IgG glycans (Table III). Sialylation appeared to be the most endogenously defined glycosylation feature, with up to 60% of variance explained by heritability. Age had very little effect on the extent of sialylation, whereas gender was nearly irrelevant. Contrary to the total plasma glycome, where gender played an important role in many glycans (68), gender was a significant predictor in the IgG glycome, although only for some structures containing bisecting GlcNAc. For the incidence of core fucose, bisecting GlcNAc and galactose, the heritability was generally between 25 and 45%, indicating that a significant part of the variability of IgG glycosylation can be explained by genetic polymorphisms.

Effects of Gender and Age—A number of strong associations between IgG glycans and age were observed and the most prominent ones are shown in Fig. 2. Individual's age was the most important predictor for the level of IgG galactosylation, with 35% of variance of G0 explained by age (Table III). This observation is in accordance with previous studies of galactosylation in aging (76, 77) and our recent study of the total plasma glycome (68). The proportion of structures with bisecting GlcNAc also increased with age, what is in accord-

ance with the results of the recent large study of IgG glycans in aging (77). However, contrary to the previous observations in plasma, the extent of core fucosylation of IgG was not found to change with age (data not shown), indicating that the observed decrease in core fucose with age in the total plasma glycome of women (68) could be the consequence of decreased IgG concentration, and not alterations in the glycosylation metabolism in plasma cells. Another difference between effects of age on glycosylation of IgG and total plasma proteins was observed in sialylation. Although in the total plasma glycome sialylation did not change with age (68), in IgG glycans there was a significant decrease of sialylation of IgG with age (Fig. 2: FGS/(F + FG + FGS)). Very recently, the logarithm of the ratio of fucosylated G0 to G2 structures (FA2/FA2G2), the so called GlycoAge index, was suggested as a good indicator of individual's age (78). In our population this index was also a reliable predictor of age with good separation of individuals in different decades of life (Fig. 3).

Acknowledgments—Plasma samples used for the isolation of IgG were collected with support of the FP6 EuroSpan project, the Royal Society, the Chief Scientist Office of the Scottish Government. We thank Carolien Koeleman for expert technical assistance, Lorraine Anderson for data collection, Dr. Eoin Cosgrave and Dr. Jonathan Bones for critical reading of the manuscript and the people of Orkney, Vis, and Korčula for volunteering.

* This work was supported by the Croatian Ministry of Science, Education, and Sport (grants #309-0061194-2023 and #216-1080315-0302), by the Croatian Science Foundation (grant # 04-47), by the European Commission (grants EuroGlycoArrays and GlycoBioM), and by the grant #P20RR017695 from the National Institute of Health, Bethesda, Maryland. In addition, M.P. gratefully acknowledges financial support of the Federation of European Biochemical Societies for her study visit to Biomolecular Mass Spectrometry Unit in Leiden and A.K. acknowledges the support of the "Unity Through Knowledge fund."

[c] To whom correspondence should be addressed: University of Zagreb, Faculty of Pharmacy and Biochemistry, A. Kovačića 1, 10000 Zagreb, Croatia. Fax: +385-1-639-4400; E-mail: glauc@pharma.hr.

REFERENCES

1. Marek, K. W., Vijay, I. K., and Marth, J. D. (1999) A recessive deletion in the GlcNAc-1-phosphotransferase gene results in peri-implantation embryonic lethality. *Glycobiology* **9,** 1263–1271
2. Dennis, J. W., Lau, K. S., Demetriou, M., and Nabi, I. R. (2009) Adaptive Regulation at the Cell Surface by N-Glycosylation. *Traffic* **10,** 1569–1578
3. Crocker, P. R., Paulson, J. C., and Varki, A. (2007) Siglecs and their roles in the immune system. *Nat. Rev. Immunol.* **7,** 255–266
4. Marth, J. D., and Grewal, P. K. (2008) Mammalian glycosylation in immunity. *Nat. Rev. Immunol.* **8,** 874–887
5. Ohtsubo, K., and Marth, J. D. (2006) Glycosylation in cellular mechanisms of health and disease. *Cell* **126,** 855–867
6. Skropeta, D. (2009) The effect of individual N-glycans on enzyme activity. *Bioorg. Med. Chem.* **17,** 2645–2653
7. Kobata, A. (2008) The N-linked sugar chains of human immunoglobulin G: their unique pattern, and their functional roles. *Biochim. Biophys. Acta* **1780,** 472–478
8. Jefferis, R. (2005) Glycosylation of recombinant antibody therapeutics. *Biotechnol. Prog.* **21,** 11–16
9. Zhu, D., Ottensmeier, C. H., Du, M. Q., McCarthy, H., and Stevenson, F. K. (2003) Incidence of potential glycosylation sites in immunoglobulin variable regions distinguishes between subsets of Burkitt's lymphoma and mucosa-associated lymphoid tissue lymphoma. *Br. J. Haematol.* **120,** 217–222
10. Parekh, R. B., Dwek, R. A., Sutton, B. J., Fernandes, D. L., Leung, A., Stanworth, D., Rademacher, T. W., Mizuochi, T., Taniguchi, T., and Matsuta, K. (1985) Association of rheumatoid arthritis and primary osteoarthritis with changes in the glycosylation pattern of total serum IgG. *Nature* **316,** 452–457
11. Kaneko, Y., Nimmerjahn, F., and Ravetch, J. V. (2006) Anti-inflammatory activity of immunoglobulin G resulting from Fc sialylation. *Science* **313,** 670–673
12. Anthony, R. M., and Ravetch, J. V. (2010) A novel role for the IgG Fc glycan: the anti-inflammatory activity of sialylated IgG Fcs. *J Clin Immunol 30 Suppl* **1,** S9–14
13. Nimmerjahn, F., and Ravetch, J. V. (2008) Fcgamma receptors as regulators of immune responses. *Nat Rev Immunol* **8,** 34–47
14. Ferrara, C., Stuart, F., Sondermann, P., Brünker, P., and Umana, P. (2006) The carbohydrate at FcgammaRIIIa Asn-162. An element required for high affinity binding to non-fucosylated IgG glycoforms. *J. Biol. Chem.* **281,** 5032–5036
15. Shinkawa, T., Nakamura, K., Yamane, N., Shoji-Hosaka, E., Kanda, Y., Sakurada, M., Uchida, K., Anazawa, H., Satoh, M., Yamasaki, M., Hanai, N., and Shitara, K. (2003) The absence of fucose but not the presence of galactose or bisecting N-acetylglucosamine of human IgG1 complex-type oligosaccharides shows the critical role of enhancing antibody-dependent cellular cytotoxicity. *J. Biol. Chem.* **278,** 3466–3473
16. Iida, S., Misaka, H., Inoue, M., Shibata, M., Nakano, R., Yamane-Ohnuki, N., Wakitani, M., Yano, K., Shitara, K., and Satoh, M. (2006) Nonfucosylated therapeutic IgG1 antibody can evade the inhibitory effect of serum immunoglobulin G on antibody-dependent cellular cytotoxicity through its high binding to FcgammaRIIIa. *Clin Cancer Res.* **12,** 2879–2887
17. Preithner, S., Elm, S., Lippold, S., Locher, M., Wolf, A., da Silva, A. J., Baeuerle, P. A., and Prang, N. S. (2006) High concentrations of therapeutic IgG1 antibodies are needed to compensate for inhibition of antibody-dependent cellular cytotoxicity by excess endogenous immunoglobulin G. *Mol. Immunol.* **43,** 1183–1193
18. Barut, M., Podgornik, A., Urbas, L., Gabor, B., Brne, P., Vidic, J., Plevcak, S., and Strancar, A. (2008) Methacrylate-based short monolithic columns: enabling tools for rapid and efficient analyses of biomolecules and nanoparticles. *J. Sep. Sci.* **31,** 1867–1880
19. Josić, D., and Buchacher, A. (2001) Application of monoliths as supports for affinity chromatography and fast enzymatic conversion. *J. Biochem. Biophys. Methods* **49,** 153–174
20. Jungbauer, A., and Hahn, R. (2008) Polymethacrylate monoliths for preparative and industrial separation of biomolecular assemblies. *J. Chromatogr. A* **1184,** 62–79
21. Roberts, M. W., Ongkudon, C. M., Forde, G. M., and Danquah, M. K. (2009) Versatility of polymethacrylate monoliths for chromatographic purification of biomolecules. *J. Sep. Sci.* **32,** 2485–2494
22. Podgornik, A., and Strancar, A. (2005) Convective Interaction Media (CIM)–short layer monolithic chromatographic stationary phases. *Biotechnol. Annu. Rev.* **11,** 281–333
23. Barut, M., Podgornik, A., Brne, P., and Strancar, A. (2005) Convective interaction media short monolithic columns: enabling chromatographic supports for the separation and purification of large biomolecules. *J. Sep. Sci.* **28,** 1876–1892
24. Brne, P., Podgornik, A., Bencina, K., Gabor, B., Strancar, A., and Peterka, M. (2007) Fast and efficient separation of immunoglobulin M from immunoglobulin G using short monolithic columns. *J. Chromatogr. A* **1144,** 120–125
25. Iberer, G., Hahn, R., and Jungbauer, A. (1999) Monoliths as stationary phases for separation of biopolymers: the fourth generation of chromatography sorbents. *LC-GC*, 998–1005
26. Urbas, L., Brne, P., Gabor, B., Barut, M., Strlic, M., Petric, T. C., and Strancar, A. (2009) Depletion of high-abundance proteins from human plasma using a combination of an affinity and pseudo-affinity column. *J. Chromatogr. A* **1216,** 2689–2694
27. Vlakh, E. G., and Tennikova, T. B. (2009) Applications of polymethacrylate-based monoliths in high-performance liquid chromatography. *J. Chromatogr. A* **1216,** 2637–2650
28. Tennikova, T. B., and Reusch, J. (2005) Short monolithic beds: history and introduction to the field. *J. Chromatogr. A* **1065,** 13–17
29. Tetala, K. K., and van Beek, T. A. (2010) Bioaffinity chromatography on

monolithic supports. *J. Sep. Sci.* **33,** 422–438
30. Berruex, L. G., Freitag, R., and Tennikova, T. B. (2000) Comparison of antibody binding to immobilized group specific affinity ligands in high performance monolith affinity chromatography. *J. Pharm. Biomed. Anal.* **24,** 95–104
31. Gupalova, T. V., Lojkina, O. V., Pàlàgnuk, V. G., Totolian, A. A., and Tennikova, T. B. (2002) Quantitative investigation of the affinity properties of different recombinant forms of protein G by means of high-performance monolithic chromatography. *J. Chromatogr. A* **949,** 185–193
32. Burnouf, T., Goubran, H., and Radosevich, M. (1998) Application of bioaffinity technology in therapeutic extracorporeal plasmapheresis and large-scale fractionation of human plasma. *J. Chromatogr. B Biomed. Sci. Appl.* **715,** 65–80
33. Rudan, I., Campbell, H., and Rudan, P. (1999) Genetic epidemiological studies of eastern Adriatic Island isolates, Croatia: objective and strategies. *Coll. Antropol.* **23,** 531–546
34. Rudan, I., Biloglav, Z., Vorko-Jović, A., Kujundzic-Tiljak, M., Stevanović, R., Ropac, D., Puntarić, D., Cucević, B., Salzer, B., and Campbell, H. (2006) Effects of inbreeding, endogamy, genetic admixture, and outbreeding on human health: a (1001 Dalmatians) study. *Croat. Med. J.* **47,** 601–610
35. Campbell, H., Carothers, A. D., Rudan, I., Hayward, C., Biloglav, Z., Barac, L., Pericic, M., Janicijevic, B., Smolej-Narancic, N., Polasek, O., Kolcic, I., Weber, J. L., Hastie, N. D., Rudan, P., and Wright, A. F. (2007) Effects of genome-wide heterozygosity on a range of biomedically relevant human quantitative traits. *Hum. Mol. Genet.* **16,** 233–241
36. Tennikova, T. B., Belenkii, B. G., and Švec, F. (1990) *J. Liq. Chromatogr.* **13,** 63–70
37. Barut, M., Podgornik, A., Merhar, M., Štrancar, A. F. Švec, T. B. Tennikova, and Z. Deyl, (2003) (Eds.), Monolithic Materials: Preparation, Properties and Applications, *Journal of Chromatography Library*, vol. 67 p. 51, Elsevier, Amsterdam.
38. Knežević, A., Polašek, O., Gornik, O., Rudan, I., Campbell, H., Hayward, C., Wright, A., Kolčić, I., O'Donoghue, N., Bones, J., Rudd, P. M., and Lauc, G. (2009) Variability, Heritability and Environmental Determinants of Human Plasma N-Glycome. *J. Proteome Res.* **8,** 694–701
39. Ahn, J., Bones, J., Yu, Y. Q., Rudd, P. M., and Gilar, M. (2010) Separation of 2-aminobenzamide labeled glycans using hydrophilic interaction chromatography columns packed with 1.7 microm sorbent. *J Chromatogr B Analyt Technol Biomed Life Sci* **878,** 403–408
40. Bones, J., Mittermayr, S., O'Donoghue, N., Guttman, A., and Rudd, P. M. (2010) Ultra performance liquid chromatographic profiling of serum N-glycans for fast and efficient identification of cancer associated alterations in glycosylation. *Anal Chem* **82,** 10208–10215
41. Ceroni, A., Maass, K., Geyer, H., Geyer, R., Dell, A., and Haslam, S. M. (2008) GlycoWorkbench: a tool for the computer-assisted annotation of mass spectra of glycans. *J. Proteome Res.* **7,** 1650–1659
42. Krapp, S., Mimura, Y., Jefferis, R., Huber, R., and Sondermann, P. (2003) Structural analysis of human IgG-Fc glycoforms reveals a correlation between glycosylation and structural integrity. *J. Mol. Biol.* **325,** 979–989
43. Berman, H. M., Westbrook, J., Feng, Z., Gilliland, G., Bhat, T. N., Weissig, H., Shindyalov, I. N., and Bourne, P. E. (2000) The Protein Data Bank. *Nucleic Acids Res.* **28,** 235–242
44. Wormald, M. R., Petrescu, A. J., Pao, Y. L., Glithero, A., Elliott, T., and Dwek, R. A. (2002) Conformational studies of oligosaccharides and glycopeptides: complementarity of NMR, X-ray crystallography, and molecular modelling. *Chem Rev* **102,** 371–386
45. Petrescu, A. J., Petrescu, S. M., Dwek, R. A., and Wormald, M. R. (1999) A statistical analysis of N- and O-glycan linkage conformations from crystallographic data. *Glycobiology* **9,** 343–352
46. Almasy, L., and Blangero, J. (1998) Multipoint quantitative-trait linkage analysis in general pedigrees. *Am. J. Hum. Genet.* **62,** 1198–1211
47. Beeck, H., and Hellstern, P. (1998) In vitro characterization of solvent/detergent-treated human plasma and of quarantine fresh frozen plasma. *Vox Sang 74* Suppl **1,** 219–223
48. Noda, K., Miyoshi, E., Uozumi, N., Yanagidani, S., Ikeda, Y., Gao, C., Suzuki, K., Yoshihara, H., Yoshikawa, K., Kawano, K., Hayashi, N., Hori, M., Taniguchi, N., and Yoshikawa, M. (1998) Gene expression of alpha1–6 fucosyltransferase in human hepatoma tissues: a possible implication for increased fucosylation of alpha-fetoprotein. *Hepatology* **28,** 944–952
49. Holland, M., Yagi, H., Takahashi, N., Kato, K., Savage, C. O., Goodall, D. M., and Jefferis, R. (2006) Differential glycosylation of polyclonal IgG, IgG-Fc and IgG-Fab isolated from the sera of patients with ANCA-associated systemic vasculitis. *Biochim. Biophys. Acta* **1760,** 669–677
50. Gornik, O., and Lauc, G. (2008) Glycosylation of serum proteins in inflammatory diseases. *Dis. Markers* **25,** 267–278
51. Fujii, S., Nishiura, T., Nishikawa, A., Miura, R., and Taniguchi, N. (1990) Structural heterogeneity of sugar chains in immunoglobulin G. Conformation of immunoglobulin G molecule and substrate specificities of glycosyltransferases. *J. Biol. Chem.* **265,** 6009–6018
52. Narasimhan, S., Freed, J. C., and Schachter, H. (1985) Control of glycoprotein synthesis. Bovine milk UDPgalactose:N-acetylglucosamine beta-4-galactosyltransferase catalyzes the preferential transfer of galactose to the GlcNAc beta 1,2Man alpha 1,3- branch of both bisected and nonbisected complex biantennary asparagine-linked oligosaccharides. *Biochemistry* **24,** 1694–1700
53. Sutton, B. J., and Phillips, D. C. (1983) The three-dimensional structure of the carbohydrate within the Fc fragment of immunoglobulin G. *Biochem. Soc Trans* **11,** 130–132
54. Lund, J., Takahashi, N., Pound, J. D., Goodall, M., and Jefferis, R. (1996) Multiple interactions of IgG with its core oligosaccharide can modulate recognition by complement and human Fc gamma receptor I and influence the synthesis of its oligosaccharide chains. *J. Immunol.* **157,** 4963–4969
55. Wormald, M. R., Rudd, P. M., Harvey, D. J., Chang, S. C., Scragg, I. G., and Dwek, R. A. (1997) Variations in oligosaccharide-protein interactions in immunoglobulin G determine the site-specific glycosylation profiles and modulate the dynamic motion of the Fc oligosaccharides. *Biochemistry* **36,** 1370–1380
56. Anthony, R. M., Nimmerjahn, F., Ashline, D. J., Reinhold, V. N., Paulson, J. C., and Ravetch, J. V. (2008) Recapitulation of IVIG anti-inflammatory activity with a recombinant IgG Fc. *Science* **320,** 373–376
57. Arnold, J. N., Wormald, M. R., Sim, R. B., Rudd, P. M., and Dwek, R. A. (2007) The impact of glycosylation on the biological function and structure of human immunoglobulins. *Annu. Rev. Immunol.* **25,** 21–50
58. Nimmerjahn, F., and Ravetch, J. V. (2006) Fcgamma receptors: old friends and new family members. *Immunity* **24,** 19–28
59. Nimmerjahn, F., and Ravetch, J. V. (2008) Anti-inflammatory actions of intravenous immunoglobulin. *Annu. Rev. Immunol.* **26,** 513–533
60. Thobhani, S., Yuen, C. T., Bailey, M. J., and Jones, C. (2009) Identification and quantification of N-linked oligosaccharides released from glycoproteins: an inter-laboratory study. *Glycobiology* **19,** 201–211
61. Wada, Y., Azadi, P., Costello, C. E., Dell, A., Dwek, R. A., Geyer, H., Geyer, R., Kakehi, K., Karlsson, N. G., Kato, K., Kawasaki, N., Khoo, K. H., Kim, S., Kondo, A., Lattova, E., Mechref, Y., Miyoshi, E., Nakamura, K., Narimatsu, H., Novotny, M. V., Packer, N. H., Perreault, H., Peter-Katalinic, J., Pohlentz, G., Reinhold, V. N., Rudd, P. M., Suzuki, A., and Taniguchi, N. (2007) Comparison of the methods for profiling glycoprotein glycans–HUPO Human Disease Glycomics/Proteome Initiative multi-institutional study. *Glycobiology* **17,** 411–422
62. Stadlmann, J., Pabst, M., Kolarich, D., Kunert, R., and Altmann, F. (2008) Analysis of immunoglobulin glycosylation by LC-ESI-MS of glycopeptides and oligosaccharides. *Proteomics* **8,** 2858–2871
63. Youings, A., Chang, S. C., Dwek, R. A., and Scragg, I. G. (1996) Site-specific glycosylation of human immunoglobulin G is altered in four rheumatoid arthritis patients. *Biochem. J.* **314** (Pt 2), 621–630
64. Shields, R. L., Lai, J., Keck, R., O'Connell, L. Y., Hong, K., Meng, Y. G., Weikert, S. H., and Presta, L. G. (2002) Lack of fucose on human IgG1 N-linked oligosaccharide improves binding to human Fcgamma RIII and antibody-dependent cellular toxicity. *J. Biol. Chem.* **277,** 26733–26740
65. Schachter, H. (1986) Biosynthetic controls that determine the branching and microheterogeneity of protein-bound oligosaccharides. *Adv. Exp. Med. Biol.* **205,** 53–85
66. Fukuta, K., Abe, R., Yokomatsu, T., Omae, F., Asanagi, M., and Makino, T. (2000) Control of bisecting GlcNAc addition to N-linked sugar chains. *J. Biol. Chem.* **275,** 23456–23461
67. Ferrara, C., Brunker, P., Suter, T., Moser, S., Puntener, U., and Umana, P. (2006) Modulation of therapeutic antibody effector functions by glycosylation engineering: influence of Golgi enzyme localization domain and co-expression of heterologous beta1, 4-N-acetylglucosaminyltransferase III and Golgi alpha-mannosidase II. *Biotechnol. Bioeng.* **93,** 851-861

68. Knežević, A., Gornik, O., Polašek, O., Pučić, M., Novokmet, M., Redžić, I., Rudd, P. M., Wright, A. F., Campbell, H., Rudan, I., and Lauc, G. (2010) Effects of aging, body mass index, plasma lipid profiles, and smoking on human plasma N-glycans. *Glycobiology* **20,** 959–969
69. Mimura, Y., Ashton, P. R., Takahashi, N., Harvey, D. J., and Jefferis, R. (2007) Contrasting glycosylation profiles between Fab and Fc of a human IgG protein studied by electrospray ionization mass spectrometry. *J. Immunol. Methods* **326,** 116–126
70. Kita, Y., Miura, Y., Furukawa, J., Nakano, M., Shinohara, Y., Ohno, M., Takimoto, A., and Nishimura, S. (2007) Quantitative glycomics of human whole serum glycoproteins based on the standardized protocol for liberating N-glycans. *Mol. Cell Proteomics* **6,** 1437–1445
71. Visscher, P. M., Hill, W. G., and Wray, N. R. (2008) Heritability in the genomics era–concepts and misconceptions. *Nat. Rev. Genet.* **9,** 255–266
72. Körner, C., Lehle, L., and von Figura, K. (1998) Carbohydrate-deficient glycoprotein syndrome type 1: correction of the glycosylation defect by deprivation of glucose or supplementation of mannose. *Glycoconjugate J.* **15,** 499–505
73. Ota, H., Nakayama, J., Momose, M., Hayama, M., Akamatsu, T., Katsuyama, T., Graham, D. Y., and Genta, R. M. (1998) Helicobacter pylori infection produces reversible glycosylation changes to gastric mucins. *Virchows Arch* **433,** 419–426
74. Tangvoranuntakul, P., Gagneux, P., Diaz, S., Bardor, M., Varki, N., Varki, A., and Muchmore, E. (2003) Human uptake and incorporation of an immunogenic nonhuman dietary sialic acid. *Proc. Natl. Acad. Sci. U.S.A.* **100,** 12045–12050
75. Barišić, K., Lauc, G., Dumić, J., Pavlović, M., and Flögel, M. (1996) Changes of glycoprotein patterns in sera of humans under stress. *Eur. J. Clin. Chem. Clin. Biochem.* **34,** 97–101
76. Parekh, R., Roitt, I., Isenberg, D., Dwek, R., and Rademacher, T. (1988) Age-related galactosylation of the N-linked oligosaccharides of human serum IgG. *J. Exp. Med.* **167,** 1731–1736
77. Ruhaak, L. R., Uh, H. W., Beekman, M., Koeleman, C. A., Hokke, C. H., Westendorp, R. G., Wuhrer, M., Houwing-Duistermaat, J. J., Slagboom, P. E., and Deelder, A. M. (2010) Decreased levels of bisecting GlcNAc glycoforms of IgG are associated with human longevity. *PLoS One* **5,** e12566
78. Vanhooren, V., Dewaele, S., Libert, C., Engelborghs, S., De Deyn, P. P., Toussaint, O., Debacq-Chainiaux, F., Poulain, M., Glupczynski, Y., Franceschi, C., Jaspers, K., van der Pluijm, I., Hoeijmakers, J., and Chen, C. C. (2010) Serum N-glycan profile shift during human ageing. *Exp. Gerontol.* **45,** 738–743